Compositional and Morphological Changes of Chemical Modified Oil Palm Mesocarp Fiber by Alkaline Bleaching and Silane Coupling Agents

Chern Chiet Eng,[a] Nor Azowa Ibrahim,[a,*] Norhazlin Zainuddin,[a] Hidayah Ariffin,[b] and Wan Md Zin Wan Yunus [c]

In this study, the effects of chemical modifications of oil palm mesocarp fiber (OPMF) *via* bleaching, silane coupling agents, and combinations of the two on the composition and morphology of OPMF were investigated. The chemically modified OPMF was characterized by Fourier transform infrared spectroscopy (FTIR), thermogravimetric analysis (TGA), and scanning electron microscopy (SEM). The FTIR spectra showed that bleached OPMF became more hydrophilic, while silanized unbleached and silanized bleached OPMF became less hydrophilic. The TGA thermograms indicated that bleaching successfully removed hemicellulose from the OPMF, while TGA analysis showed that silanized unbleached and silanized bleached OPMF had higher thermal stabilities than unbleached or bleached OPMF. The SEM micrographs revealed that the modified OPMF surface was rougher and more porous than that of the unbleached OPMF, further indicating that OPMF was successfully modified.

Keywords: Oil palm mesocarp fiber; Chemical modification; Bleaching; Silane coupling agent

*Contact information: a: Department of Chemistry, Faculty of Science, University Putra Malaysia, 43400 UPM Serdang, Selangor, Malaysia; b: Department of Bioprocess Technology, Faculty of Biotechnology and Biomolecular Sciences, University Putra Malaysia, 43400 UPM Serdang, Selangor, Malaysia; c: Chemistry Department, Centre for Defence Foundation Studies, National Defence University of Malaysia, Kem Sungai Besi, 57000 Kuala Lumpur, Malaysia; *Corresponding author: norazowa@upm.edu.my*

INTRODUCTION

The oil palm (*Elaeis guineensis*) originates from South Africa, grows well in all tropical areas of the world, and has become one of the main industrial crops of Malaysia. The Malaysian palm oil industry has grown tremendously over the last 25 years, and Malaysia has become the world's leading producer and exporter of palm oil (Mohammed *et al*. 2011). Generally, oil palm biomass products are produced from plantations and mills. Biomass from plantations is primarily trunk and fronds, whereas biomass from mills consists of empty fruit bunches (EFB), mesocarp fibers, palm kernel shells, and palm oil mill effluent (POME) (Abas *et al*. 2011). For every kilogram of palm oil produced, approximately four kilograms of dry biomass are produced, excluding palm oil mill effluent (POME). In 2010, the amount of mesocarp fiber available was 10.80 Mt/year (Ng *et al*. 2012). Thus, there is a huge amount of fiber that can be used instead of being discarded as waste. Traditionally, the mesocarp fiber is mixed with kernel shells and is used as a solid fuel to generate electricity for the mill.

Natural fiber as reinforcement filler in polymer composites has received increasing attention from researchers because natural fibers have many significant advantages over

synthetic fibers. They are environmentally friendly, fully biodegradable, renewable, cheap, and have low density (Wambua *et al*. 2003). However, there are some disadvantages such as poor wettability, incompatibility with some polymeric matrices, and high moisture adsorption which restrict their usage in polymer composites (Riccieri *et al*. 1999). To make natural, hydrophilic fibers more compatible with hydrophobic polymer matrices, the fibers can be modified to enhance their interfacial adhesion. Chemical modification of natural fibers exposes more reactive groups on the fiber surface and thus promotes more efficient coupling with a polymer matrix (Dash *et al*. 2000). Chemical modifications such as alkali treatment (Alam *et al*. 2012), acetylation treatment (Bledzki *et al*. 2008), isocyanate treatment (George and Verpoest 1999), treatment with maleated coupling agents (Mohanty *et al*. 2004), treatment with silane coupling agents (Abdelmouleh *et al.* 2007), grafting (Ibrahim *et al.* 2005), and surface deposition of multiwall carbon nanotubes (MWCNTs) (Tzounis *et al*. 2014) have been conducted to improve fiber-matrix adhesion.

Alkali-treated fiber may form alkali-resistant linkages between lignin and hemicellulose, impeding the removal of lignin. Hydrogen peroxide can be used to break these linkages and delignify the fibers to promote interfacial adhesion with the polymer matrix (Salam *et al*. 2007). Hydrogen peroxide can also remove cementing materials from the fiber which block adhesion with the polymer matrix. Under alkaline conditions, hydroxyl ions (OH^-) produced by the perhydroxyl ion (HO_2^-) hydrolyze hydrogen ions (H^+), liberating more perhydroxyl ions. Perhydroxyl ions may decompose into hydroxyl ions and atomic oxygen where the atomic oxygen is responsible for bleaching (Modibbo *et al*. 2009). Due to the problem that colours of the natural fiber are mainly brown or dark brown, which are not attractive to consumer, bleaching of the natural fiber by hydrogen peroxide is an applicable approach to make the natural fiber/ polymer composites more attractive and marketable.

Silane coupling agents are multifunctional molecules used to modify the surface of natural fibers. Chemical bonding theory is the most accepted theory explaining the interfacial bonding mechanisms of silane coupling agents. In chemical bonding theory, bifunctional silane molecules form chemical linkages between the matrix and the fibers *via* a chemical bond with the fiber surface through a siloxane bridge. Their organofunctional group simultaneously bonds to the polymer matrix. The general chemical formula of silane is X_3Si-*R*, where *R* represents a group that can react with the matrix and *X* represents a group that can hydrolyze to form a silanol group in aqueous solution and react with the hydroxyl groups of the fiber surface; the *R*-group can be vinyl-, aminopropyl-, methacreloxypropyne- (and others) while the *X*-group can be chloro-, methoxy-, ethoxy- (and others). Silane undergoes several stages of hydrolysis, condensation, and bond formation during the modification of fibers. When the silane-bonded fiber surface connects with the matrix, the *R*-groups on the fiber surface react with the functional groups of the polymer matrix to form stable covalent bonds with the matrix. Thus, silane coupling agents function as bridges between fibers and the matrix (Herrera Franco and Valadez-González 2005). Therefore, silane-treated fiber are able to improve fiber/matrix adhesion between silane-treated fiber with polymer matrix.

The major goal of the modification of OPMF by combination of alkali bleaching and silane coupling agent is to produce a suitable, cheap, and compatible OPMF-based reinforcement filler in expensive biodegradable polymer matrix. The modified OPMF is expected to improve the fiber/matrix adhesion between modified fiber and polymer matrix which eventually produce a composite with reasonable good strength and properties that are comparable with some conventional plastics while at the same time also lowering the

cost of biodegradable polymer. The applications of the composites might be more suitable for single use materials that do not require very high strength; at the same time biodegradability is important for the selection of materials.

The objective of this study was to investigate the effects of chemical modification of OPMF and the changes in the composition of OPMF following bleaching, application of silane coupling agents, and the combination of these two methods. We hypothesized that the alkali bleaching of OPMF will make the surface of OPMF become rough and porous which would be possibly more favourable as a pretreatment before silanization. This is because bleaching exposure of more hydroxyl groups enables more extensive interaction between OPMF with silane. The modified OPMF was characterized by Fourier transform infrared spectroscopy (FTIR), thermogravimetric analysis (TGA), and scanning electron microscopy (SEM).

EXPERIMENTAL

Materials

All reactions were carried out using reagent-grade chemicals (greater than 98% purity) without further purification. Raw oil palm mesocarp fibers were obtained from Felda Palm Ind., Sdn Bhd., Serting Hilir, Negeri Sembilan. Sodium hydroxide was supplied by Merck (Germany), hydrogen peroxide from J. T. Baker (USA), and 3-(Trimethoxysilyl) propyl methacrylate from Acros Organic (USA).

Methods

Processing of raw OPMF

The raw OPMF fiber was soaked in distilled water for 24 h to remove impurities. It was then rinsed with hot water (60 °C) twice and finally with acetone to remove wax prior to drying at 60 °C in an air oven. The fiber was ground and sieved to a particle size of 150 μm using a crusher machine.

Modification of OPMF by alkaline bleaching

The OPMF was soaked in a solution containing a 1:1 ratio of 5% sodium hydroxide and 10% hydrogen peroxide for 2 h. The pH of the solution was maintained at approximately 11. The bleached OPMF was washed with distilled water and dried at 60 °C in an air oven overnight.

Modification of OPMF by methacrylate silane

First, 5 wt.% silane (weight percentage compared to OPMF) was dissolved for hydrolysis in a mixture of a 3:2 ratio of ethanol and water. The pH of the solution was adjusted to 4 with acetic acid, and the mixture was stirred continuously for an hour. Then, unbleached or bleached OPMF was soaked in the solution for 3 h and dried at 60 °C in an air oven overnight.

Fourier transform infrared spectroscopy (FTIR)

A Perkin Elmer Spectrum 100-series spectrometer (USA) equipped with an attenuated total reflectance (ATR) unit was used to evaluate the functional groups and types of bonds present in the samples. The infrared spectra were recorded in the range of 280 to 4000 cm^{-1}.

Thermogravimetric analysis (TGA)

A Perkin Elmer TGA7 apparatus (USA) was used for the thermogravimetic analysis of the samples. Samples of about 15 mg were heated from 35 to 1000 °C with a heating rate of 10 °C/min. Nitrogen gas was pumped through the apparatus at a flow rate of 20 mL/min to maintain an inert nitrogen atmosphere.

Scanning electron microscopy (SEM)

The surface morphology of modified OPMF was observed with a scanning electron microscope (JEOL JSM-6400, Japan) after the samples were sputter-coated with gold using a Bio-rad (USA) coating system.

RESULTS AND DISCUSSION

Fourier Transform Infrared Spectroscopy (FTIR)

The FTIR spectra of unbleached and bleached OPMF are shown in Fig. 1. The peak at 1723 cm^{-1} for the unbleached OPMF corresponds to carbonyl group stretching, predominantly due to the acid and ester functional groups of hemicellulose (Proniewicz *et al.* 2002). The carbonyl group stretching peak disappeared from the bleached OPMF spectra because of the splitting of the ester groups of hemicellulose by alkaline hydrolysis (Agarwal and McSweeny 1997). This indicates that bleaching removes all hemicellulose from the OPMF. The peaks at 1628 and 1638 cm^{-1} in the spectra of unbleached and bleached OPMF correspond to C=C stretching**.** The peak at 1238 cm^{-1} in the spectrum of unbleached OPMF, corresponding to C-O stretching, disappeared after bleaching, perhaps due to the removal of hemicellulose from the OPMF. The H-bonded O-H stretching, represented by the peaks at 3339 cm^{-1} (unbleached) and 3337 cm^{-1} (bleached), show that OPMF is hydrophilic in nature. The increment in the absorbance of bleached OPMF is due to the removal of oxidized carbohydrates and lignin. The phenyl -OH groups of lignin and COOH/COONa groups of carbohydrates undergo further degradation under alkaline conditions (Wójciak *et al*. 2010). Thus, bleached OPMF became more hydrophilic than unbleached OPMF.

The FTIR spectra of silanized unbleached and silanized bleached OPMF are illustrated in Fig. 2. The peaks at 3335 and 3338 cm^{-1} represent H-bonded O-H stretching for silanized unbleached and silanized bleached OPMF, respectively. The decrement in the intensities of both peaks compared to those of unbleached and bleached OPMF indicates a reduction in the hydrophilicity OPMF following silase treatment. This was due to the reaction of fiber with the alkoxy functional groups of silane (Singh *et al*. 1998). The hydrolysis of silane forms silanol, which reacts with the -OH groups of fibers to form stable, covalent bonds to the cell wall. These bonds are chemisorbed onto the fiber surface, thus reducing their hydrophilicity (Huda *et al*. 2008). The peaks representing carbonyl stretching (at 1721 cm^{-1}) and C-O stretching (at 1252 cm^{-1}), present in the spectrum of silanized unbleached OPMF, disappeared from the silanized bleached OPMF spectrum due to the removal of hemicellulose *via* bleaching. The peaks at 1160 and 1157 cm^{-1} were attributed to the asymmetric stretching of -Si-O-Si or -Si-O-C- bonds present in silanized unbleached and silanized bleached OPMF, respectively. The -Si-O-Si bonds indicate the existence of polysiloxanes deposited on the fiber, while -Si-O-C- bonds indicate the condensation reaction between silane and fibers (Pothan *et al*. 2006).

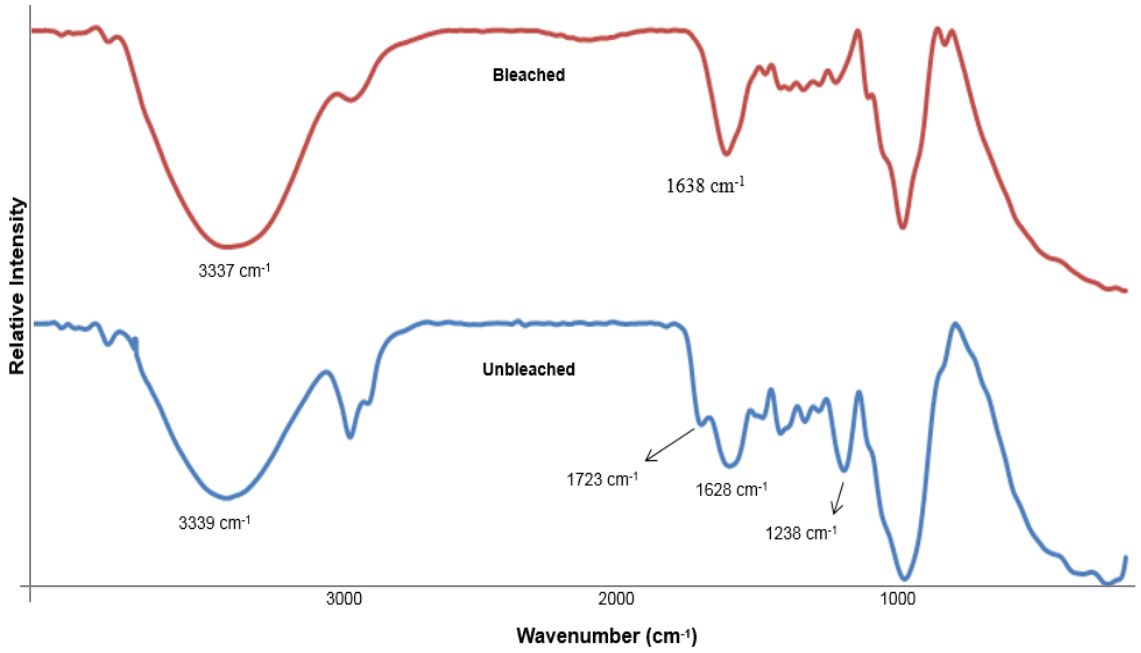

Fig. 1. FTIR spectra of unbleached and bleached OPMF

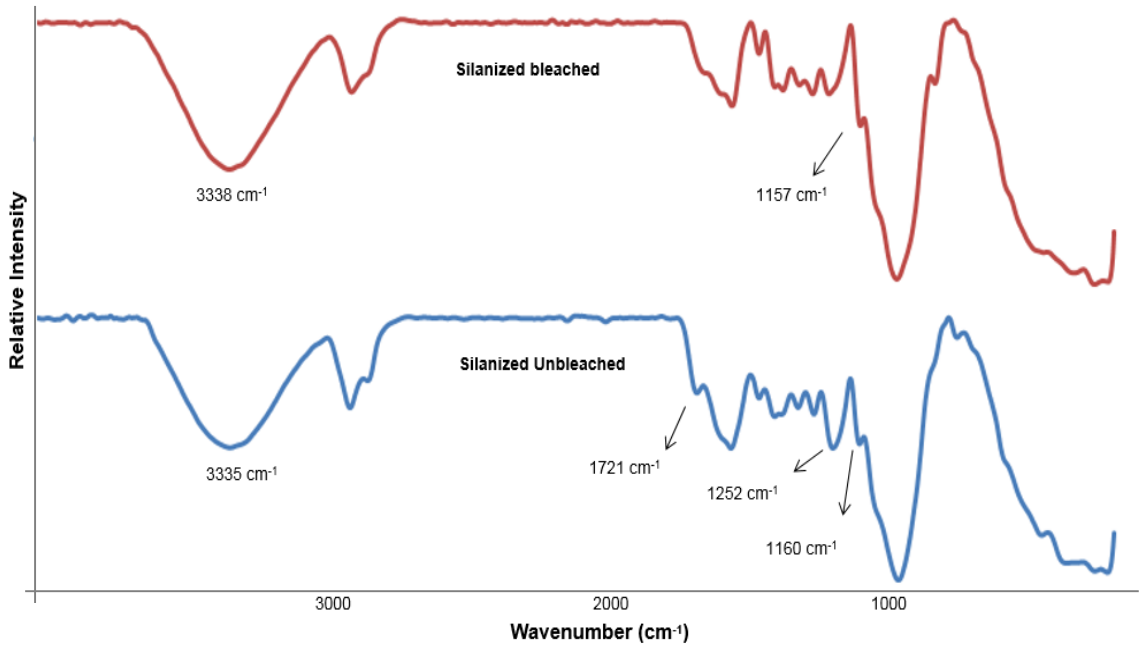

Fig. 2. FTIR spectra of silanized unbleached and silanized bleached OPMF

Thermogravimetric Analysis (TGA)

The TG thermograms for unbleached and bleached OPMF are shown in Fig. 3. The thermal degradation of both types of fiber was a gradual process with two main steps in their respective TG curves, similarly to those of other lignocellulosic compounds (Ruseckaite and Jiménez 2003). Thermal degradation of hemicellulose began at around 180 °C and reached a maximum rate at around 280 °C (Lv *et al*. 2010). Cellulose decomposed throughout the temperature range of 240 to 390 °C, while lignin decomposed

slowly at low temperatures and at a maximum degradation rate at approximately 900 °C (Vamvuka *et al*. 2003). Initial weight losses of about 3.58% and 2.69% at around 140 °C for unbleached and bleached OPMF, respectively, corresponded to the volatilization of absorbed moisture present in the fiber (Ciannamea *et al*. 2010).

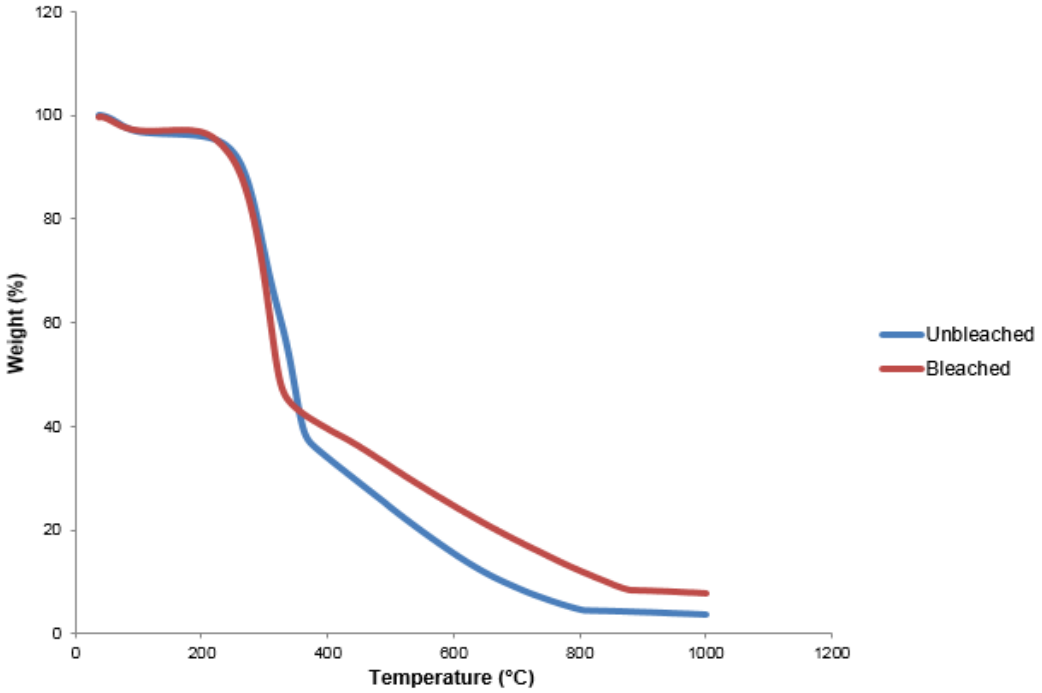

Fig. 3. TG thermogram of unbleached and bleached OPMF

The DTG thermogram in Fig. 4 shows that the thermal decomposition of unmodified OPMF was a 3-stage process.

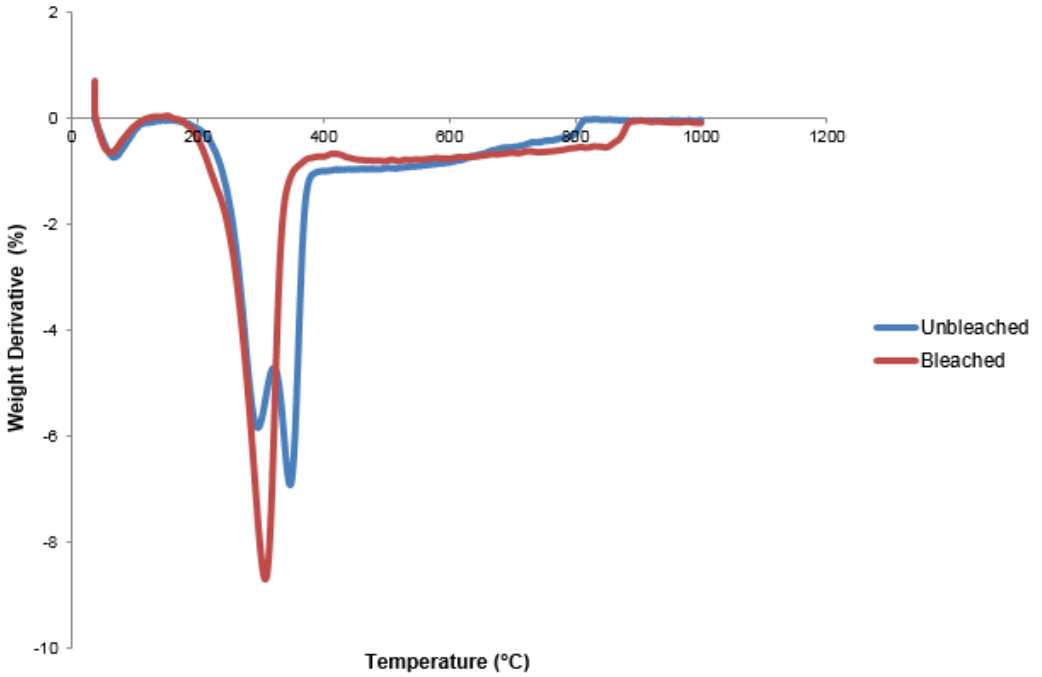

Fig. 4. DTG thermogram of unbleached and bleached OPMF

The first stage took place within the temperature range of 140 to 300 °C; the second, from 300 to 410 °C; and the third, in which the maximum degradation rate was achieved, at around 820 °C. Thermal decomposition of bleached OPMF was a 2-stage process with stages at temperatures ranging from approximately 130 to 410 °C and 410 to 900 °C. According to Stefani *et al*. (2005), depolymerisation of hemicellulose and amorphous cellulose occurs fastest at a temperature of about 300 °C. Random cleavage of the glycosidic linkage remaining in cellulose occurs until around 400 °C. This suggests that bleaching the OPMF successfully removed part of the hemicellulose and amorphous cellulose, as the degradation peak disappeared from the DTG thermogram. The degradation of unbleached and bleached OPMF at temperatures above 400 °C was mainly *via* the degradation of lignin over a broad temperature range. The char yields for unmodified and bleached fiber were 4 and 9%, respectively, as the inorganic nutrients in plants become char (Van De Velde and Kiekens 2002). Table 1 lists the thermal degradation temperatures and weight losses of unbleached and bleached OPMF.

Table 1. Thermal Degradation of Unbleached and Bleached OPMF

Sample	Temperature (°C)	Weight Loss (%)	Degraded Component
Unbleached	35 to 140	3.58	Moisture
	140 to 300	22.87	Hemicellulose, cellulose, lignin
	300 to 400	40.05	Cellulose, lignin
	400 to 820	28.78	Lignin
	820 to 1000	4.72	Char
Bleached	35 to 130	2.69	Moisture
	130 to 410	58.53	Cellulose, lignin
	410 to 900	30.32	Lignin
	900 to 1000	8.46	Char

The TG and DTG thermograms for silanized unbleached and silanized bleached OPMF are shown in Figs. 5 and 6, respectively. The thermal analysis shows that silanized unbleached and silanized bleached OPMF were more thermally stable than unbleached and bleached OPMF, respectively. Both categories of silane-treated fibers had greater thermal stability, which is in agreement with the findings of Arbelaiz *et al*. (2006). The initial weight losses of about 4.96 and 7.58% occurred at around 120 °C for silanized unbleached and silanized bleached OPMF, respectively. These small weight losses were attributed to absorbed moisture present in the fiber. The DTG thermogram shows that the thermal decomposition of silanized unbleached OPMF was mainly a 3-stage process taking place in temperature ranges of 120 to 340 °C, 340 to 490 °C, and with maximum degradation temperature at around 900 °C. This temperature was higher than that for unbleached OPMF. The thermal decomposition of silanized bleached OPMF was a 2-stage process taking place throughout temperature ranges of approximately 120 to 500 °C and 500 to 950 °C, also higher than those of bleached OPMF. The thermal degradation stages of both types of silane-treated OPMF are shown in Tables 4 and 5. The char yields from silanized unbleached and silanized bleached OPMF were around 4.1 and 9.6%, respectively. Due to the complex structure of lignin, it is difficult for all of the reactive sites of lignin react to with silane, which could be one of the reasons why the thermal degradation of lignin at temperatures above 500 °C was a 2-step process for both types of silane-treated OPMF. The first step of the degradation, the degradation of unreacted lignin, took place from

around 500 to 800 °C. The second step of the degradation took place from 800 to 900 °C and might be due to the degradation of OPMF strongly bonded to silane *via* siloxane bridges, imparting the lignin with greater thermal stability. Table 2 lists the thermal degradation temperatures and weight losses of silanized unbleached and silanized bleached OPMF.

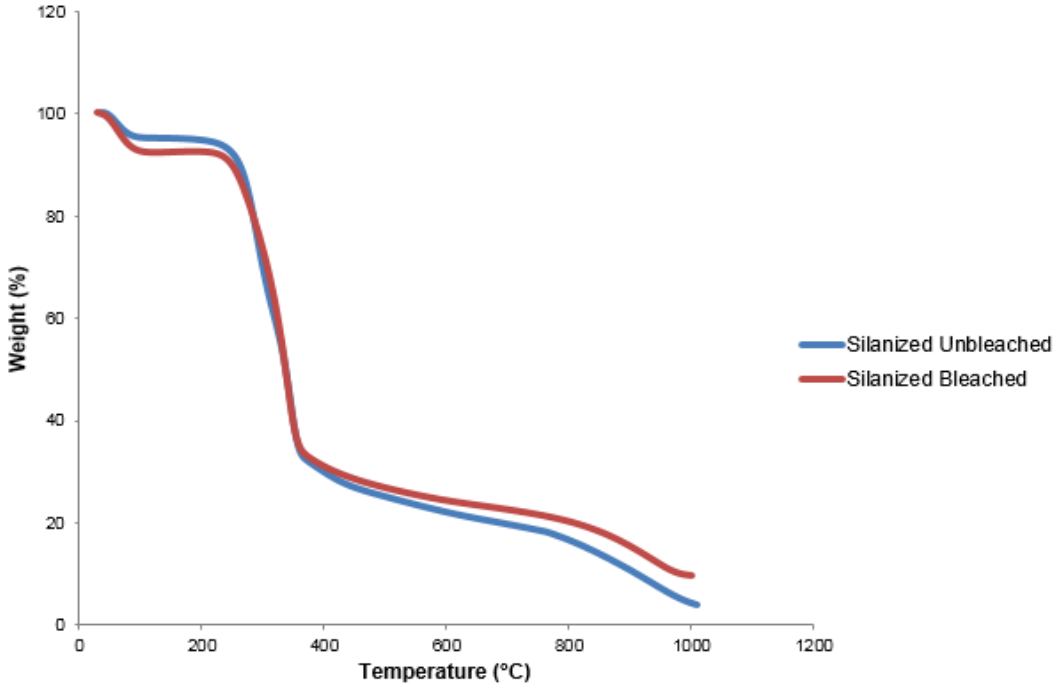

Fig. 5. TG thermogram of silanized unbleached and silanized bleached OPMF

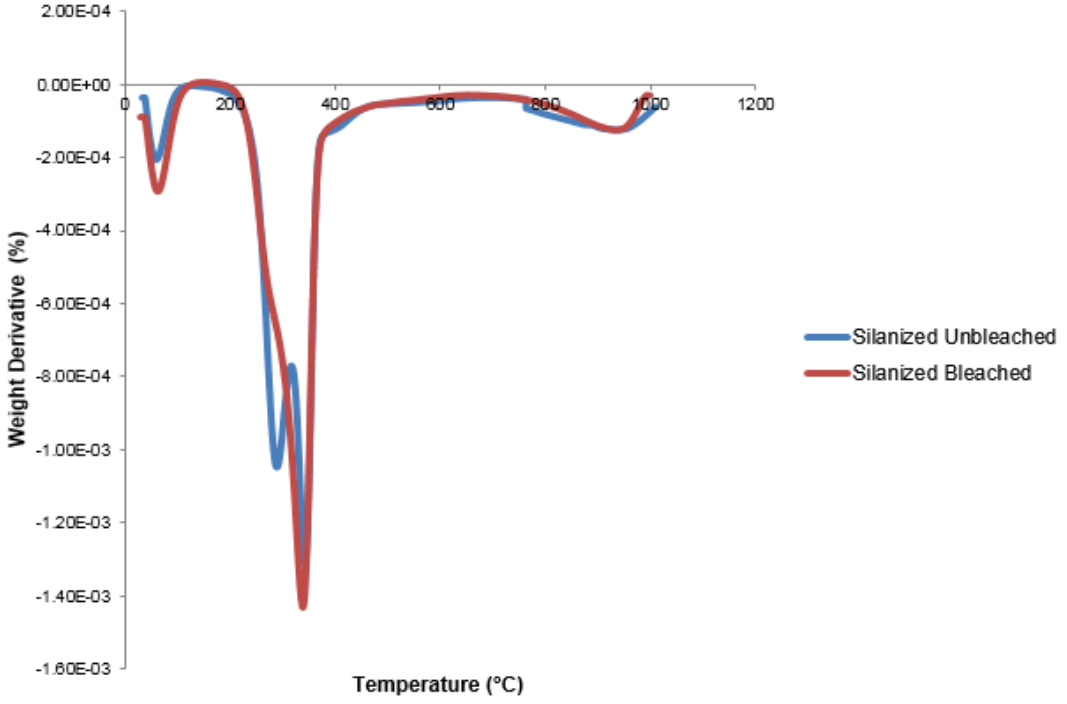

Fig. 6. DTG thermogram of silanized unbleached and silanized bleached OPMF

Table 2. Thermal Degradation of Silanized Unbleached and Silanized Bleached OPMF

Sample	Temperature (°C)	Weight Loss (%)	Degraded Component
Silanized unbleached	35 to 120	4.96	Moisture
	120 to 340	35.05	Hemicellulose, cellulose, lignin
	340 to 490	29.66	Cellulose, lignin
	490 to 900	30.33	Lignin
	900 to 1000	4.06	Char
Silanized bleached	35 to 120	7.58	Moisture
	120 to 500	60.42	Cellulose, lignin
	500 to 950	22.40	Lignin
	950 to 1000	9.60	Char

Scanning Electron Microscopy (SEM)

Figure 7 shows SEM micrographs of (a) unbleached OPMF and (b) bleached OPMF. Figure 7a shows that the surface of unbleached OPMF was smooth and sleek with no signs of external fibrillation or fibrils. Figure 7b shows that the surface of bleached OPMF was rough and heterogeneous with many pores. This indicates that bleached OPMF was in the process of peeling and underwent morphological changes (Roncero *et al*. 2005). The SEM results agree with the TGA results; lignocellulosic components were removed after bleaching, leading to greater exposure of hydroxyl groups and favoring chemical interactions with the polymer matrix.

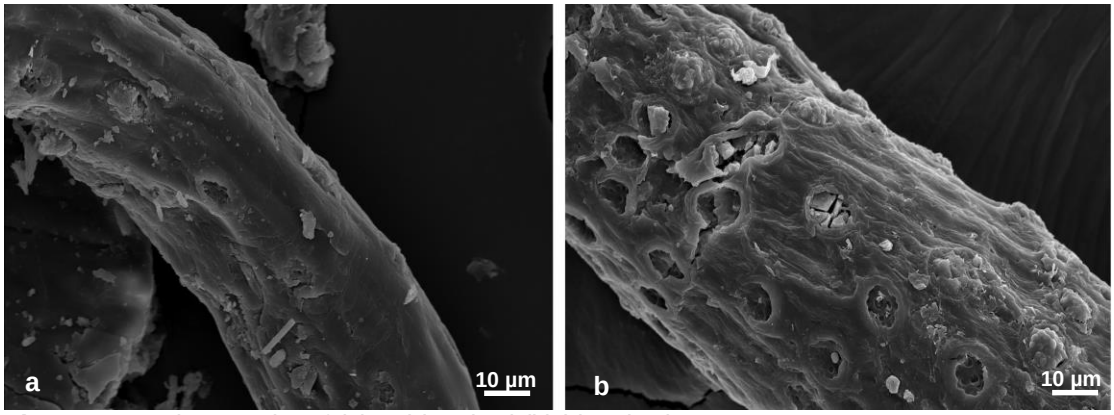

Fig. 7. SEM micrographs of (a) unbleached (b) bleached OPMF

The SEM micrographs of silanized unbleached and silanized bleached OPMF are shown in Fig. 8. Figure 8a shows that the surface of silanized unbleached OPMF was rough and had many pores. Similarly, the surface of silanized bleached OPMF, as shown in Fig. 8b, was also rough and heterogeneous, with many pores. However, the pores present on the surface of silanized bleached OPMF were much deeper and larger than those of the silanized unbleached OPMF. This is because bleaching exposed more hydroxyl groups and enabled more interaction with silane which thus support the hypothesis that bleaching as pretreatment before silanization was more favourable as silane coupling are more easily to react with OH group that expose on the fiber surface.

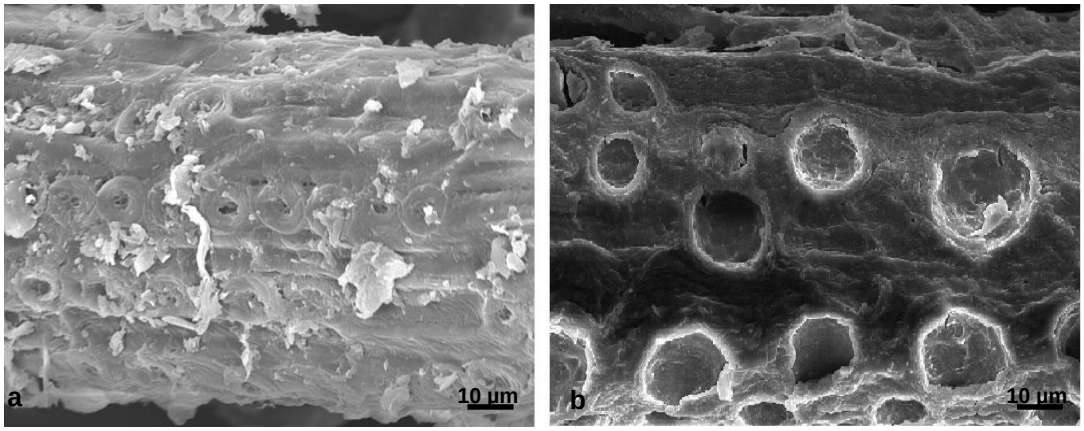

Fig. 8. SEM micrographs of (a) silanized unbleached (b) silanized bleached OPMF

CONCLUSIONS

1. The FTIR spectra and TGA thermograms showed that alkaline peroxide bleaching of OPMF successfully removed hemicellulose from its fibers.
2. The SEM micrographs showed that the surface of bleached OPMF was rougher with more pores than that of the unbleached OPMF, which was smooth.
3. Unbleached and bleached OPMF were treated with silane coupling agents. The FTIR spectra indicated that the silanized unbleached and silanized bleached OPMF were less hydrophilic than unbleached and bleached OPMF.
4. The TGA thermograms showed that both types of silane-treated OPMF had greater thermal stability than the unbleached and bleached OPMF.
5. The SEM micrographs revealed that the pores on the surface of silanized bleached OPMF surface were much deeper and larger than those on the surface of silanized unbleached OPMF. This was due to bleaching's exposure of more hydroxyl groups, enabling more extensive interaction with silane.

ACKNOWLEDGMENTS

The authors would like to thank the Research University Grant Scheme (RUGS) of UPM for financial support. The technical staff of the Department of Chemistry, Faculty of Science, Universiti Putra Malaysia are thanked for their assistance.

REFERENCES CITED

Abas, R., Kamaruddin, M. F., Nordin, A. B. A., and Simeh, M. A. (2011). "A study on the Malaysian oil palm biomass sector - Supply and perception of palm oil millers," *Oil Palm Industry Economic Journal* 11(1), 28-41.

Abdelmouleh, M., Boufi, S., Belgacem, M. N., and Dufresne, A. (2007). "Short natural-fibre reinforced polyethylene and natural rubber composites: Effect of silane coupling agents and fibres loading," *Composites Science and Technology* 67(7-8), 1627-1639.

Agarwal, U. P., and McSweeny, J. D. (1997). "Photoyellowing of thermomechanical pulps: Looking beyond α-carbonyl and ethylenic groups as the initiating structures," *Journal of Wood Chemistry and Technology* 17(1-2), 1-26.

Alam, M. A. K. M., Beg, M. D. H., Prasad, R. D. M., Khan, M. R., and Mina, M. F. (2012). "Structures and performances of simultaneous ultrasound and alkali treated oil palm empty fruit bunch fiber reinforced poly(lactic acid) composites," *Composites Part A: Applied Science and Manufacturing* 43(11), 1921-1929.

Arbelaiz, A., Fernández, B., Ramos, J. A., and Mondragon, I. (2006). "Thermal and crystallization studies of short flax fibre reinforced polypropylene matrix composites: Effect of treatments," *Thermochimica Acta* 440(2), 111-121.

Bledzki, A. K., Mamun, A. A., Lucka-Gabor, M., and Gutowski, V. S. (2008). "The effects of acetylation on properties of flax fibre and its polypropylene composites," *eXPRESS Polymer Letters* 2(6), 413-422.

Ciannamea, E. M., Stefani, P. M., and Ruseckaite, R. A. (2010). "Medium-density particleboards from modified rice husks and soybean protein concentrate-based adhesives," *Bioresource Technology* 101(2), 818-825.

Dash, B. N., Rana, A. K., Mishra, S. C., Mishra, H. K., Nayak, S. K., and Tripathy, S. S. (2000). "Novel low-cost jute–polyester composite. II. SEM observation of the fractured surfaces," *Polymer-Plastics Technology and Engineering* 39(2), 333-350.

George, J., and Verpoest, J. I. I. (1999). "Mechanical properties of flax fibre reinforced epoxy composites," *Die Angewandte Makromolekulare Chemie* 272(1), 41-45.

Herrera Franco, P. J., and Valadez-González, A. (2005). "Fiber-matrix adhesion in natural fiber composites," in: *Natural Fibers, Biopolymers, and Biocomposites*, Mohanty, A. K. , Misra, M., and Drzal, L. T., eds. CRC Press, Boca Raton, FL, pp. 180-236.

Huda, M. S., Drzal, L. T., Mohanty, A. K., and Misra, M. (2008). "Effect of fiber surface-treatments on the properties of laminated biocomposites from poly(lactic acid) (PLA) and kenaf fibers," *Composites Science and Technology* 68(2), 424-432.

Ibrahim, N., Abu-Ilaiwi, F., Rahman, M., Ahmad, M., Dahlan, K., and Yunus, W. (2005). "Graft copolymerization of acrylamide onto oil palm empty fruit bunch (OPEFB) fiber," *Journal of Polymer Research* 12(3), 173-179.

Lv, G. J., Wu, S. B., and Lou, R. (2010). "Kinetic study for the thermal decomposition of hemicellulose isolated from corn stalk," *BioResources* 5(2), 1281-1291.

Modibbo, U. U., Aliyu, B. A., and Nkafamiya, I. I. (2009). "The effect of mercerization media on the physical properties of local plant bast fibres," *International Journal of Physical Sciences* 4(11), 698-704.

Mohammed, M. A. A., Salmiaton, A., Wan Azlina, W. A. K. G., Mohammad Amran, M. S., Fakhru'l-Razi, A., and Taufiq-Yap, Y. H. (2011). "Hydrogen rich gas from oil palm biomass as a potential source of renewable energy in Malaysia," *Renewable and Sustainable Energy Reviews* 15(2), 1258-1270.

Mohanty, S., Nayak, S. K., Verma, S. K., and Tripathy, S. S. (2004). "Effect of MAPP as a coupling agent on the performance of jute-PP composites," *Journal of Reinforced Plastics and Composites* 23(6), 625-637.

Ng, W. P. Q., Lam, H. L., Ng, F. Y., Kamal, M., and Lim, J. H. E. (2012). "Waste-to-wealth: Green potential from palm biomass in Malaysia," *Journal of Cleaner Production* 34, 57-65.

Pothan, L. A., Thomas, S., and Groeninckx, G. (2006). "The role of fibre/matrix interactions on the dynamic mechanical properties of chemically modified banana

fibre/polyester composites," *Composites Part A: Applied Science and Manufacturing* 37(9), 1260-1269.

Proniewicz, L. M., Paluszkiewicz, C., Weselucha-Birczynska, A., Baranski, A., and Dutka, D. (2002). "FT-IR and FT-Raman study of hydrothermally degraded groundwood containing paper," *Journal of Molecular Structure* 614(1), 345-353.

Riccieri, J. E., Vázquez, A., and De Carvalho, L. H. (1999). "Interfacial properties and initial step of the water sorption in unidirectional unsaturated polyester/vegetable fiber composites," *Polymer Composites* 20 (1), 29-37.

Roncero, M. B., Torres, A. L., Colom, J. F., and Vidal, T. (2005). "The effect of xylanase on lignocellulosic components during the bleaching of wood pulps," *Bioresource Technology* 96(1), 21-30.

Ruseckaite, R. A., and Jiménez, A. (2003). "Thermal degradation of mixtures of polycaprolactone with cellulose derivatives," *Polymer Degradation and Stability* 81(2), 353-358.

Salam, A., Reddy, N., and Yang, Y. (2007). "Bleaching of kenaf and cornhusk fibers," *Industrial & Engineering Chemistry Research* 46(5), 1452-1458.

Singh, B., Verma, A., and Gupta, M. (1998). "Studies on adsorptive interaction between natural fiber and coupling agents," *Journal of Applied Polymer Science* 70(9), 1847-1858.

Stefani, P. M., Garcia, D., Lopez, J., and Jimenez, A. (2005). "Thermogravimetric analysis of composites obtained from sintering of rice husk-scrap tire mixtures," *Journal of Thermal Analysis and Calorimetry* 81(2), 315-320.

Tzounis, L., Debnath, S., Rooj, S., Fischer, D., Mäder, E., Das, A., Stamm, M., and Heinrich, G. (2014). "High performance natural rubber composites with a hierarchical reinforcement structure of carbon nanotube modified natural fibers," *Materials & Design* 58, 1-11,

Vamvuka, D., Kakaras, E., Kastanaki, E., and Grammelis, P. (2003). "Pyrolysis characteristics and kinetics of biomass residuals mixtures with lignite," *Fuel* 82(15-17), 1949-1960.

Van De Velde, K., and Kiekens, P. (2002). "Thermal degradation of flax: The determination of kinetic parameters with thermogravimetric analysis," *Journal of Applied Polymer Science* 83(12), 2634-2643.

Wambua, P., Ivens, J., and Verpoest, I. (2003). "Natural fibres: can they replace glass in fibre reinforced plastics?" *Composites Science and Technology* 63(9), 1259-1264.

Wójciak, A., Kasprzyk, H., Sikorska, E., Khmelinskii, I., Krawczyk, A., Oliveira, A. S., and Sikorski, M. (2010). "Changes in chromophoric composition of high-yield mechanical pulps due to hydrogen peroxide bleaching under acidic and alkaline conditions," *Journal of Photochemistry and Photobiology A: Chemistry* 215(2-3), 157-163.

Article submitted: April 3, 2014; Peer review completed: July 8, 2014; Revised version received and accepted: July 9, 2014; Published: July 17, 2014.